

Acceleration of cone-produced electrons by double-line Ti-sapphire laser beating

Cite as: Phys. Plasmas **19**, 053106 (2012); <https://doi.org/10.1063/1.4707390>

Submitted: 15 February 2012 • Accepted: 27 March 2012 • Published Online: 16 May 2012

Y. Mori and Y. Kitagawa



View Online



Export Citation

ARTICLES YOU MAY BE INTERESTED IN

[Controlling the betatron oscillations of a wakefield-accelerated electron beam by temporally asymmetric laser pulses](#)

Phys. Plasmas **18**, 043107 (2011); <https://doi.org/10.1063/1.3577566>

[Autoinjection of electrons into a wake field using a capillary with attached cone](#)

Phys. Plasmas **16**, 123103 (2009); <https://doi.org/10.1063/1.3271152>

[Self-focusing of short intense pulses in plasmas](#)

The Physics of Fluids **30**, 526 (1987); <https://doi.org/10.1063/1.866349>



Physics of Plasmas
Features in Plasma Physics Webinars

Register Today!

Acceleration of cone-produced electrons by double-line Ti-sapphire laser beating

Y. Mori^{a)} and Y. Kitagawa

The Graduate School for the Creation of New Photonics Industries, 1955-1 Kurematsucho, Nishiku, Hamamatsu, Shizuoka 431-1202, Japan

(Received 15 February 2012; accepted 27 March 2012; published online 16 May 2012)

Acceleration of electrons is demonstrated in a beat wave scheme by using a prepulse-free short-pulse (150 fs) double-line Ti-sapphire laser. To inject electrons, we used a hybrid target composed of a cone-drilled plate and a gas jet, where the cone-produced electrons were accelerated via the forced plasma wave excited in the gas jet that was situated behind the plate. This resulted in an increase in slope temperature from 0.05 to 0.15 MeV. We find a correlation between the slope temperature and forced relativistic plasma wave. The wake amplitude is 15 GV/m at the resonant density of $2.5 \times 10^{18} \text{ cm}^{-3}$ in a hydrogen plasma. The wake acceleration models can explain the increase in slope temperature. © 2012 American Institute of Physics. [<http://dx.doi.org/10.1063/1.4707390>]

I. INTRODUCTION

The concept of a laser-plasma accelerator¹ has been demonstrated for ns-pulse double-line CO₂ lasers for self-trapping electrons in a plasma² and for the external injection of electrons from a radio-frequency linear accelerator.³ In addition, a ps-pulse CO₂ laser beat wave has been used to accelerate injected electrons into a 3-cm-long plasma wave.⁴ Combining a chirped-pulse-amplified (CPA) laser with a capillary,⁵ 1 GeV monoenergetic electrons have been accelerated.^{6,7} These recent results imply the need for more powerful lasers such as a petawatt laser. However, as long as a single-pulse laser drives the wake field, even a bubble/blowout regime,^{8,9} further improvements are required to provide a stable and controllable accelerator. This is because both (i) injection and (ii) acceleration of electrons should be accomplished in a single-stage. In the single-stage, since so-called self-injection occurs through transverse wave breaking,¹⁰ it is challenging for a fine control of electron bunch. This wave breaking also causes some modulation into the designed wake field amplitude.

When we applied a staging scheme,¹¹ conversely, we can separate (i) injection and (ii) acceleration and control them individually. Especially, if we focus on (ii) acceleration, a pulse train from the laser beat wave drives the forced excitation of a stable wake field, as required by stable accelerators. In combination with stable electron injectors,^{12–16} the forced wake field by beat wave can be a candidate for stable wake field driver.

To address the forced wake field acceleration by laser beating, we apply a simple scheme to simultaneously inject and accelerate electrons. To inject electrons, we use a hybrid target composed of a cone-drilled plate and a gas jet, where the cone-produced electrons are accelerated via the forced plasma wave excited in the gas jet, which is situated behind the plate. The double-line short-pulse laser generates and injects electrons through the solid cone and simultaneously accelerates them in the beat-wave-forced wake field.

In this paper, we present our scheme for simultaneously injecting and accelerating electrons, which is accomplished by a double-line Ti-sapphire laser beating and a hybrid target. Section II describes the experimental setup and results including the beat laser system, experimental setup, forced-wake-field detection, and acceleration of electrons by a hybrid target. Section III gives our analysis of the experimental results, which indicates that acceleration can be explained from a wake model. Finally, we discuss the results in Sec. IV and conclude in Sec. V.

II. EXPERIMENTAL SETUP AND RESULTS

A. Double-line Ti-sapphire beat laser

To ensure that a few beating pulse bunches will be of the required pulse duration, we have developed a double-line Ti-sapphire laser system¹⁷ with a pulse duration of 150 fs and a beat period τ_{beat} of 72 fs, which corresponds to a resonant electron density of $2.5 \times 10^{18} \text{ cm}^{-3}$. Figure 1 shows schematics of BEAT laser and provided pulse shape and spectrum. Pulses from two oscillators, centered at wavelengths of 785 and 815 nm, are overlapped spatially and temporally and injected into an optical parametric CPA (OPCPA),¹⁸ resulting in a prepulse-free 150 fs, 180 mJ output. Here, we operated the laser in two different modes: First is the double-line mode, which activates two oscillators to produce a beating trace in the pulse, as shown in Fig. 1. This mode enables the beat wave operation. The second mode is the single-line mode, which activates only a single oscillator, resulting in a single pulse trace without beating in the pulse. In the double-line operation, as shown in Fig. 2(a), the second-order autocorrelation image shows that the 150 fs pulse is modulated at the beat period τ_{beat} of 72 fs, in agreement with the beat period evaluated from the spectral separation $\Delta\lambda = 30 \text{ nm}$ shown in (b).

Figure 3 shows experimental setup for beat wave electron acceleration. As illustrated in Fig. 3(a), the laser beam is focused by an off-axis parabolic mirror. The forced relativistic plasma wave is excited in the hydrogen gas jet when the

^{a)}Electronic mail: ymori@gpi.ac.jp.

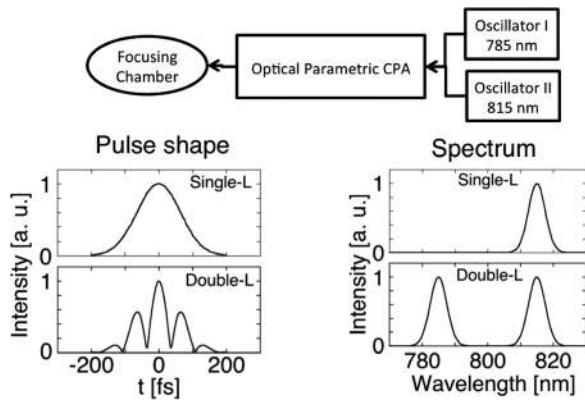


FIG. 1. Schematics of BEAT laser and provided pulse shape and spectrum for “single-line” and “double-line” operations.

beat frequency (ω_b : $\Delta\omega = \omega_1 - \omega_2$) is getting close to the electron plasma frequency ω_{pe} , where ω_1 and ω_2 are the frequencies of the laser pulses.

B. Evaluation of wake-field amplitude

In this section, we evaluate the amplitude of the wake field in hydrogen plasma driven by the beating laser that is focused at the center of the free-expansion hydrogen-gas jet. The laser energy was 80 mJ, the pulse duration was 200 fs, and the focal spot size was $13 \mu\text{m}$. The intensity I of $3 \times 10^{17} \text{ W/cm}^2$ corresponds to $a_0 = 0.38$. The Rayleigh range was $250 \mu\text{m}$.

The free-expansion hydrogen-gas jet was generated by a commercial pulsed valve (General Valve Series 9) with a 2-mm-diameter orifice. The electron density profile along the laser irradiation direction is measured by a shearing interferometer. Here, the leakage from the compressed beam is converted into a wavelength of 407 nm and is used to probe the gas jet plasma perpendicularly to the laser pulse.¹⁹ The electron density profile along the laser irradiation direction is shown in Fig. 4. The dashed curve is a fitting to eye guide. The peak density is $1.1 \times 10^{19} \text{ cm}^{-3}$ when the backing pressure P is 10 atm. Since the Rayleigh range was $250 \mu\text{m}$, from Fig. 4, we confirm that the electron density profile at the intense laser interaction region can be uniform.

The plasma-wave excitation was confirmed by the scattered laser light in the higher-harmonic sidebands, detected with an imaging 16-bit CCD spectrometer (Acton

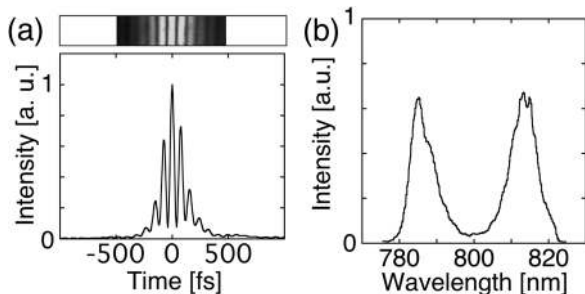


FIG. 2. (a) Second-order autocorrelation image (upper) and trace (bottom) of the double-line (785 and 815 nm) laser. The full width half maximum is 150 fs and $\tau_{beat} = 72$ fs. (b) Laser spectrum.

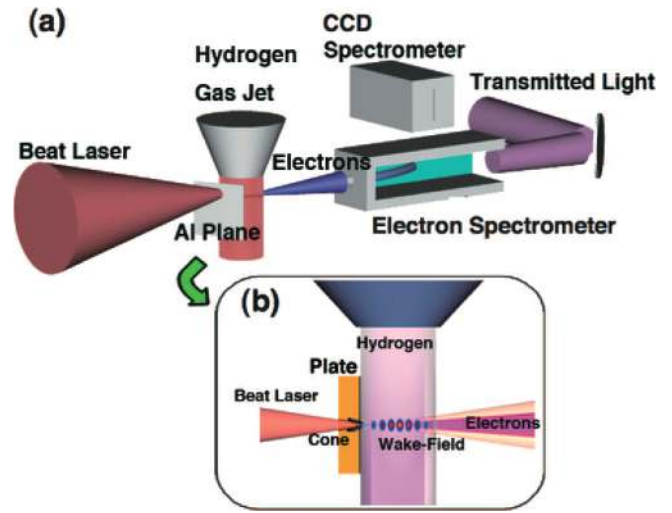


FIG. 3. Experimental setup for beat wave electron acceleration: (a) overview, (b) magnification of the hybrid target, combining an Al plate and a hydrogen-gas jet.

InSpectrum 300). The spectral resolution was 0.04 nm/pixel, and the incident light was reduced to less than $2.0 \times 10^6 \text{ W/cm}^2$ to avoid nonlinear effects in the window material.

Figure 5(a) shows the variation of the normalized sideband intensities I_1/I_0 versus backing pressure P or normalized electron density n_e/n_{res} (solid circles). Here, $n_e/n_{res} = 1.0$ is given at $P = 2.2$ atm assuming from Fig. 4 that this electron density varied linearly with the backing pressure from the vacuum. I_0 is the main peak at 815 nm and I_1 is the sideband peak between 843 and 846 nm, as shown in Fig. 4(b). This sideband corresponds the first Stokes ($\omega_2 - \omega_b$). The error bars show the average deviation over five shots. No sideband peak is detected without a gas jet, which shows that nonlinear effects in the optical measurement system were negligible. In addition, when we operate the laser as “single-line” mode in which a single pulse trace without beating in the pulse, no sideband peak was detected. This indicates that the forced wake-field is not excited without the laser beating.

In Fig. 5(b), the solid circles give the wave amplitude ϵ versus the backing pressure P or normalized electron density

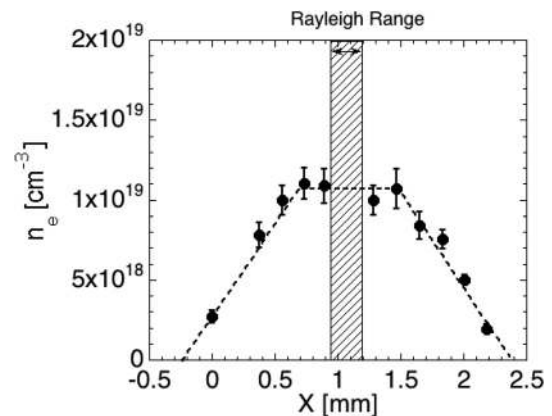


FIG. 4. Electron density profile along the laser irradiation direction. The backing pressure is 10 atm.

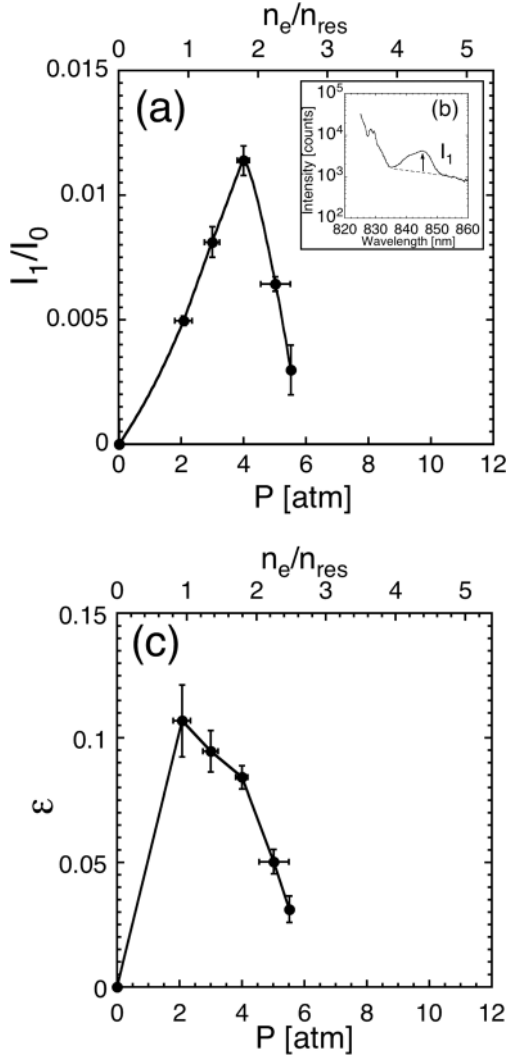


FIG. 5. (a) Variation of normalized sideband intensities I_1/I_0 versus backing pressure P or normalized electron density n_e/n_{res} (solid circles). (b) Sideband peak spectrum intensity scattered around 845 nm: I_1 . (c) Variation of wave amplitude ϵ versus P or n_e/n_{res} (solid circles).

n_e/n_{res} . This wave amplitude is evaluated from the normalized sideband intensities. For a small amplitude, I_1/I_0 can be expressed as

$$I_1/I_0 = 1/16[(\omega/c)(n_e/n_{cr})\epsilon L]^2, \quad (1)$$

where ω is the laser frequency, c is the speed of light, n_{cr} is the critical electron density, $\epsilon = \Delta n_e/n_e$ is the modulated wave amplitude, and L is the laser propagation distance.²⁰ If we assume L is the Rayleigh range Z_R , ϵ becomes 0.1 at $n_e/n_{res} = 1$ and this ϵ drops to 0.05 at $n_e/n_{res} = 2$ as shown in Fig. 5(b). The acceleration gradient is 15 GV/m at $n_e/n_{res} = 1$. In this experiment, the accelerated electrons were below the detection limit of our electron spectrometer.

C. Acceleration of electrons by hybrid target

To inject electrons into the wake field, we introduced a plate-gas hybrid target composed of an aluminum plate 500 μm thick placed in front of a gas jet, as shown in Fig. 3(b). The laser was focused 2 mm below the gas nozzle

on the rear surface of the plate. In a sequence of 100 laser-pulse shots irradiating a fresh surface, the first 30 shots drilled a cone structure into the Al plate and the remaining 70 shots went through the plate into the gas flow. The electrons produced by the cone wall flowed into the wake field, excited by the same laser beating. Because the Rayleigh range was 250 μm , we expected that the laser, which penetrated through the rear surface of the plate into the gas, would have sufficient intensity to drive the wake field. The laser intensity I was $8 \times 10^{17} \text{ W/cm}^2$, which corresponds to a normalized vector potential $a_0 = 0.62$. Sentoku *et al.* simulated the cone-structure production of relativistic electrons along the cone surface.²¹ Furthermore, Mori *et al.* reported their experimental result in which these electrons were trapped in a wake field.²² They demonstrated it by a gaussian laser pulse. We applied this scheme for the forced wake field excited by laser beating.

The electron spectrometer was set 150 mm from the focal point along the irradiation axis and consisted of a 35 mT permanent dipole magnet and an imaging plate [(IP) Fuji Film: BAS-SR 2025]. The entrance consisted of a 5-mm-diameter aperture. The energy range of the electrons was from 0.05 to 1.2 MeV. The detection limit was $dN/dE/d\Omega = 10^6$ electrons/MeV/Sr. We used the sensitivity curve of the IP reported in Ref. 23.

Figure 6 represents the energy distribution of electrons for the plate target (no gas flow behind the plate) and hybrid target (plate target and gas flow) under beat wave operation. The backing pressure of the gas jet was set to resonate plasma-wave excitation for laser beating. The laser irradiated the aluminum plate surface and drilled a cone through it. At $dN/dE/d\Omega = 2 \times 10^7$ electrons/MeV/Sr, an electron energy of 0.7 MeV for the plate target increases to 1.2 MeV for the hybrid target. This is explained as the 0.7 MeV injected seed electrons being accelerated to 1.2 MeV.

The detection limit made it difficult to trap higher-energy electrons. Without the plate target, neither the beat wave nor the single-line operations yield detectable electron signals, as indicated by the arrow labeled “Gas” in the figure.

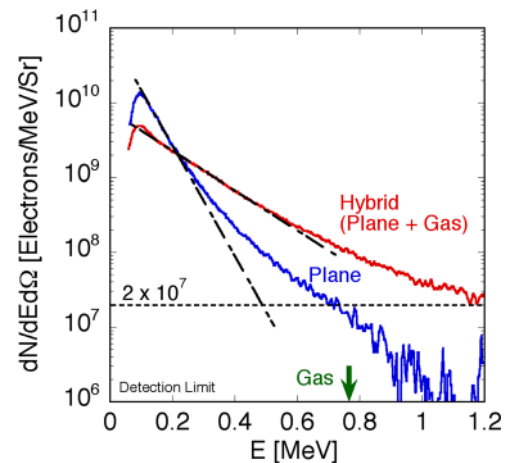


FIG. 6. Energy distribution of electrons for plate target (blue) and hybrid target (red) under beat wave operation. The dashed-dotted curves represent $dN/dE = N/T_e \exp(-E/T_e)$, as a function of slope temperatures T_e . For the gas target without the plate target, electrons are below the detection limit.

This result indicates that, combining the gas-jet with plate, the laser-excited wake field can accelerate the electrons, provided there are enough of them injected.

In Fig. 6, we focus on the slope of the spectrum for both targets, which seems to indicate acceleration effects. The dashed-dotted curve represents $dN/dE = N/T_e \exp(-E/T_e)$ (above 0.1 MeV), which is a function of slope temperature T_e . For the hybrid target, T_e increases from 0.05 to 0.15 MeV given for only plate target.

Figure 7 shows the correlation between T_e and the backing pressure or normalized electron density for the hybrid target. The solid circles represent the variation under “double-line” or beat wave operation. The fitting curve shows that T_e has a peak at $n_e/n_{res} = 1.5$. The displacement from the resonance density: $n_e/n_{res} = 1$ might be because the laser interacted with the edge of gas jet where the electron density is lower than that of center required higher gas pressure to satisfy the forced beat wave condition. Under single-line operation (open circles), the fitting curve indicates an absence of peak in T_e . In both cases, the error bars represent the uncertainty arising from electron transmittance through the electron-collimating aperture of the electron spectrometer. For the case where there is no gas ($P = 0$ atm), the temperature of the accelerated electrons is different when single-line is compared to the double-line shot. It is supposed that the beat wave operation has several bunches in the pulse; therefore, a prior bunch produces over-dense plasma and remaining bunches interact with this over-dense plasma resulting in high slope-temperature. In contrast, for the single-line operation, the single pulse interacts with a solid-surface rather than the over-dense plasma resulting in low slope-temperature because the BEAT is pre-pulse free.

For $P > 10$ atm, T_e has a dispersion from the fitting. In this region, since the electron density is beyond 10^{19} cm^{-3} , the acceleration mechanism is achieved possibly by a self-modulation rather than the beat wave. For the beat wave, the slope temperature T_e shows a peak around the resonant electron density. This peak is not observed for single-line operation as shown in Fig. 7.

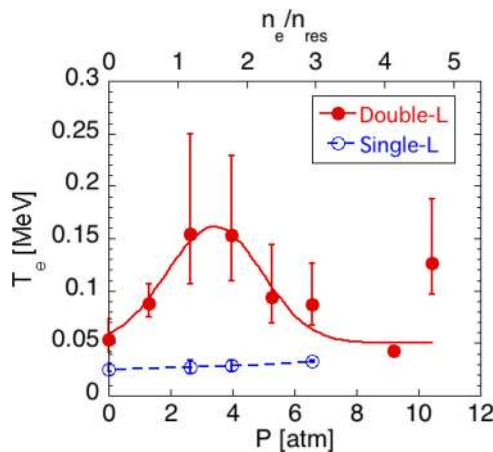


FIG. 7. Variation of T_e versus backing pressure P or normalized electron density n_e/n_{res} under beat wave (solid circles) and single-line (open circles) operation with a hybrid target.

III. RESULTS AND ANALYSIS

From the previous results, as shown in Figs. 5 and 7, beat wave operations show the forced incremental of the slope temperature T_e and the sideband intensity I_1/I_0 in relation to the backing gas pressure or electron density. As shown in Fig. 8(a), T_e has increments in relation to I_1/I_0 , indicating that the slope temperature has a correlation with the wake amplitude ϵ , that is, $\propto \sqrt{I_1/I_0}/n_e$.

In Fig. 8(b), the closed circles show the increment of T_e against ϵ . The solid curve comes from the relativistic kinetic equation of motion given in Eq. (2), which assumes that electrons absorb energy from the wake during an acceleration phase $\xi = 0 \sim \pi$,²⁴

$$d(\gamma\beta)/dt = -(eE_w/m_e c) \sin(\xi + \phi_0). \quad (2)$$

Here, γ and β are the energy and velocity of the electron, respectively, and m_e is the mass in the wave frame. $E_w = eE_{wb}$ is the amplitude of the wake field and ϕ_0 is the initial phase relative to the wake. E_{wb} is the wake field of the wave-breaking limit.

The slope temperature is evaluated from the gain difference between electrons having an initial energy separation of 50 keV (a value obtained experimentally). This model shows that the slope temperature increases as the wake amplitude increases. Therefore, T_e can be associated with the wake-field acceleration both qualitatively and quantitatively.

In this model, for $\epsilon < 0.24$, electrons experience both acceleration and deceleration as they travel the acceleration length. When $\epsilon > 0.24$, electrons can be trapped by the wake and thereby experience, within the acceleration distance, acceleration with no deceleration.

IV. DISCUSSION

Using the femtosecond ultra-intense laser beating, we have produced forced-plasma-wave excitation. As determined by side-band measurements of the scattered laser light, the wave amplitude is $\epsilon = 0.1$ and the acceleration gradient is 15 GV/m at the resonant density. However, we could not detect the accelerated electrons with this target setup, i.e., the gas jet without a plate, because the electron density was too low to yield a sufficient number of accelerated electrons. Moreover, at the resonant electron density with a laser

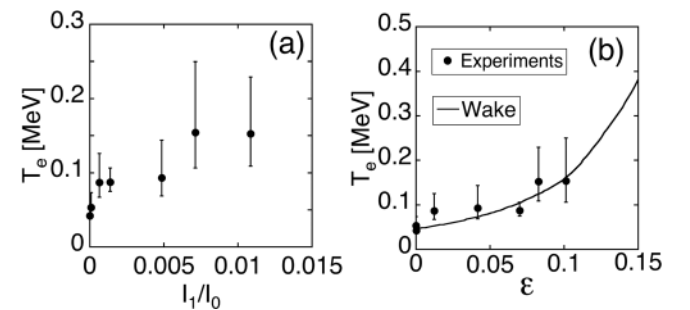


FIG. 8. (a) Variation of slope temperature T_e versus normalized sideband intensities I_1/I_0 under beat wave operation. (b) T_e against wave amplitude ϵ under beat wave operation. The solid curve is from a theory that assumes that electrons absorb energy from the wake during an acceleration phase.²⁴

intensity of $a_0 = 0.38$, the wake-field (plasma-wave) amplitude $\epsilon = 0.1$ was far below the threshold at which the wake can trap electrons from the bulk plasma. The minimum trapping energy W_{min} was found to be 1.5 MeV.² This energy is higher than that expected from the laser ponderomotive force,²⁵ which is $T_{hot} = (\sqrt{1 + a_0^2} - 1)m_e c^2 = 36$ keV. Therefore, to accelerate electrons using forced-plasma-wave excitation, both higher-density and higher-energy electrons should be injected into the wake field. Here, these electrons are supplied from the cone-drilled plate. Using a 10 TW CPA Nd:glass laser beat, Walton *et al.* generated a plasma wave with a beat wave period τ_{beat} of 700 fs.^{26,27} However, they did not give the electron acceleration, which might have been because injection was not achieved with their experimental setup. Here, we show the acceleration of electrons by femtosecond laser beating by using a plate-gas hybrid target in which, via the forced plasma wave, cone-produced electrons from the plate are accelerated in the gas jet that is situated behind the plate. The acceleration increases their slope temperature from 0.05 to 0.15 MeV.

Because the phase velocity of the wake is much faster than the electron velocity, the electrons experience both acceleration and deceleration as they travel the length of the wake field (commonly given by the Rayleigh range). Electrons below W_{min} are not trapped in the wake potential but are modulated or heated by it. In Sec. III, analysis of slope-temperature increases can be associated with wake-field acceleration both qualitatively and quantitatively. This analysis accounts only for the acceleration phase and gives its maximum; nevertheless, it explains well the experimental results.

By using femtosecond laser beating, we excited a plasma wave of beyond 10 GV/m (or $\epsilon \sim 0.1$) with no electron acceleration from the bulk plasma at the electron density of 10^{18} cm⁻³. This result means that the laser beating may be used as a dark-current-free plasma acceleration cavity. For a single-pulse wake-field acceleration scheme, a higher laser intensity is required to increase the wake-field amplitude, which also implies self-injection of electrons from the bulk plasma.

Consider the situation where we develop a dark-current-free laser wake-field accelerator in combination with an external injector and multi-staging wake acceleration cavities. The driving laser for such an acceleration cavity would require a moderate-intensity laser (i.e., with sufficiently high intensity to create a wake field yet with sufficiently low intensity to sustain self-injection). Laser beating can satisfy these conditions by multibunching and forced wake-field oscillation with a moderate peak intensity.

V. CONCLUSIONS

We have demonstrated the acceleration of electrons in a beat wave scheme that uses a short-pulse (150 fs) double-line Ti-sapphire laser. The wake amplitude is 15 GV/m at the resonant density of 2.5×10^{18} cm⁻³ in a hydrogen plasma. To inject electrons, we used a plate-gas hybrid target in which, via the forced plasma wave, cone-produced electrons from the plate are accelerated in the gas jet that is

situated behind the plate, increasing their slope temperature from 0.05 to 0.15 MeV. This increase in slope temperature is explained by wake acceleration. Laser-beating can also be used for dark-current-free plasma acceleration by the forced-wake-field oscillations.

ACKNOWLEDGMENTS

This work was supported by the Advanced Compact Accelerator Development Project of the Ministry of Education, Culture, Sports, Science and Technology and the National Institute of Radiological Sciences, Japan, Grants-in-Aid for Scientific Research from MEXT Nos. 20740323 and 22740366, 2008~2010 Grants of the Science Research Promotion Fund of the Promotion and Mutual Aid Corporation for Private Schools of Japan. The authors wish to thank K. Mima and Y. Sakawa, ILE, Osaka University, for the ILE-GPI collaboration research #B2-4I, and K. Kondo, JAEA, and S. Nakai, GPI.

¹T. Tajima and J. M. Dawson, *Phys. Rev. Lett.* **43**, 207 (1979).

²Y. Kitagawa, T. Matsumoto, T. Minamihata, K. Sawai, K. Matsuo, K. Mima, K. Nishihara, H. Azechi, K. A. Tanaka, H. Takabe, and S. Nakai, *Phys. Rev. Lett.* **68**, 48 (1992).

³C. E. Clayton, K. A. Marsh, A. Dyson, M. Everett, A. Lai, W. P. Leemans, R. Williams, and C. Joshi, *Phys. Rev. Lett.* **70**, 37 (1993).

⁴S. Ya. Tochitsky, R. Narang, C. V. Filip, P. Miisumeci, C. E. Clayton, R. B. Yoder, K. A. March, J. B. Rosenzweig, C. Pellegrini, and C. Joshi, *Phys. Rev. Lett.* **92**, 095004 (2004).

⁵Y. Kitagawa, Y. Sentoku, S. Akamatsu, W. Sakamoto, R. Kodama, K. A. Tanaka, K. Azumi, T. Norimatsu, T. Matuoka, H. Fujita, and H. Yoshida, *Phys. Rev. Lett.* **92**, 205002 (2004).

⁶W. P. Leemans, B. Nagler, A. J. Gonsalves, Cs. Tóth, K. Nakamura, C. G. R. Geddes, E. Esarey, C. B. Schroeder, and S. M. Hooker, *Nat. Phys.* **2**, 690 (2006).

⁷K. Nakamura, B. Nagler, Cs. Tóth, C. G. R. Geddes, C. B. Schroeder, E. Esarey, A. J. Gonsalves, S. M. Hooker, and W. P. Leemans, *Phys. Plasmas* **14**, 056708 (2007).

⁸A. Pukhov and J. Meyer-ter-Vehn, *Appl. Phys. B* **74**, 355 (2002).

⁹W. Lu, C. Huang, M. Zhou, W. B. Mori, and T. Katsouleas, *Phys. Rev. Lett.* **96**, 165002 (2006).

¹⁰S. V. Bulanov, F. Pegoraro, A. M. Pukhov, and A. S. Sakharov, *Phys. Rev. Lett.* **78**, 4205 (1997).

¹¹B. B. Pollock, C. E. Clayton, J. E. Ralph, F. Albert, A. Davidson, L. Divol, C. Filip, S. H. Glenzer, K. Herpoldt, W. Lu, K. A. Marsh, J. Meinecke, W. B. Mori, A. Pak, T. C. Rensink, J. S. Ross, J. Shaw, G. R. Tynan, C. Joshi, and D. H. Froula, *Phys. Rev. Lett.* **107**, 045001 (2011).

¹²J. Faure, C. Rechatin, A. Norlin, A. Lifschitz, Y. Glinec, and V. Malka, *Nature* **444**, 737 (2006).

¹³C. G. R. Geddes, K. Nakamura, G. R. Plateau, Cs. Toth, E. Cormier-Michel, E. Esarey, C. B. Schroeder, J. R. Cary, and W. P. Leemans, *Phys. Rev. Lett.* **100**, 215004 (2008).

¹⁴J. Faure, C. Rechatin, O. Lundh, L. Ammoura, and V. Malka, *Phys. Plasmas* **17**, 083107 (2010).

¹⁵A. Pak, K. A. Marsh, S. F. Martins, W. Lu, W. B. Mori, and C. Joshi, *Phys. Rev. Lett.* **104**, 025003 (2010).

¹⁶C. McGuffey, A. G. R. Thomas, W. Schumaker, T. Matsuoka, V. Chvykov, F. J. Dollar, G. Kalintchenko, V. Yanovsky, A. Maksimchuk, K. Krushelnick, V. Y. Bychenkov, I. V. Glazyrin, and A. V. Karpeev, *Phys. Rev. Lett.* **104**, 025004 (2010).

¹⁷Y. Mori, S. Fukumochi, Y. Hama, K. Kondo, Y. Sentoku, and Y. Kitagawa, *Int. J. Mod. Phys. B* **21**, 572 (2007).

¹⁸H. Yoshida, E. Ishii, R. Kodama, H. Fujita, Y. Kitagawa, Y. Izawa, and T. Yamanaka, *Opt. Lett.* **28**, 257 (2003).

¹⁹Y. Mori, H. Kuwabara, K. Ishii, R. Hanayama, T. Kawashima, and Y. Kitagawa, *Appl. Phys. Express* **5**, 056401 (2012).

²⁰R. E. Slusher and C. M. Surko, *Phys. Fluid* **23**, 472 (1980).

²¹Y. Sentoku, K. Mima, H. Ruhl, Y. Toyama, R. Kodama, and T. E. Cowan, *Phys. Plasmas* **11**, 3083 (2004).

- ²²Y. Mori, Y. Sentoku, K. Kondo, K. Tsuji, N. Nakaii, S. Fukumochi, M. Kashihara, K. Kimura, K. Takeda, K. A. Tanaka, T. Norimatsu, T. Tanimoto, H. Nakamura, M. Tampo, R. Kodama, E. Miura, K. Mima, and Y. Kitagawa, *Phys. Plasmas* **16**, 123103 (2009).
- ²³K. A. Tanaka, T. Yabuuchi, T. Sato, R. Kodama, Y. Kitagawa, T. Takahashi, and S. Okuda, *Rev. Sci. Instrum.* **76**, 013507 (2005).
- ²⁴N. A. Ebrahim and S. R. Douglas, *Laser Part. Beams* **13**, 147 (1995).
- ²⁵S. C. Wilks, *Phys. Fluids B* **5**, 2603 (1993).
- ²⁶B. Walton, Z. Najmudin, M. S. Wei, C. Marle, R. J. Kingham, K. Krushelnick, A. E. Dangor, R. J. Clarke, M. J. Poulter, C. Hernandez-Gomez, S. Hawkes, D. Neely, J. L. Collier, C. N. Danson, S. Fritzler, and V. Malka, *Opt. Lett.* **27**, 2203 (2002).
- ²⁷B. Walton, Z. Najmudin, M. S. Wei, C. Marle, R. J. Kingham, K. Krushelnick, A. E. Dangor, R. J. Clarke, M. J. Poulter, C. Hernandez-Gomez, S. Hawkes, D. Neely, J. L. Collier, C. N. Danson, S. Fritzler, and V. Maika, *Phys. Plasmas* **13**, 013103 (2008).